Contents list available at IJRED website

International Journal of Renewable Energy Development

Journal homepage: https://ijred.undip.ac.id

Research Article

MATLAB/Simulink Based Instantaneous Solar Radiation Modeling, Validation and Performance Analysis of Fixed and Tracking Surfaces for the Climatic Conditions of Lahore City, Pakistan

Naseer Ahmad*

Department of Mechanical Engineering, University of Engineering and Technology Lahore, Pakistan

Abstract. Mathematical modeling, simulation and experimental validation of instantaneous solar radiation is conducted in this article. The input parameters of the developed model are solar constant, latitude & longitude of the selected site, collector surface azimuth and elevation angle. The whole model is developed in MATLAB/Simulink and plots global radiation for any selected day of the year. To validate the model, actual data from RETScreen (energy management software) is taken and compared with the predicted data from developed model. During the whole year the predicted specific insolation is 226.65 MJ/m²/day and actual is 202.14 MJ/m²/day. The percentage error of the predicted data is 10.8% higher than the actual data. The validated model is used to calculate the monthly received solar radiation energy for the fixed surface and tracking surface. The yearly harvested solar energy by horizontal, yearly and monthly optimal tilt surfaces are 6828 MJ/m², 7405 MJ/m² and 7761 MJ/m² respectively. Yearly insolation gain of the yearly optimal tilt and monthly optimal tilt collector surface is 8% and 14% as compared to the energy harvested by horizontal surface. For the single and dual axis tracking surfaces, yearly harvested energy is 8843 MJ/m² and 9374 MJ/m² respectively and this figure is 30% and 37% more as compared to the horizontal surface. If the insolation received by yearly optimal tilt is considered as reference value, then energy gain for monthly tilt, single and dual axis tracking is recorded as 5%, 19% and 27% respectively.

Keywords: Solar Radiation, Modeling, Performance analysis, Tracking Systems

Received: 1st June 2021; Revised: 20th Feb 2022; Accepted: 4th April 2022; Available online: 15th April 2022

1. Introduction

The world energy demand can be satisfied by the enormous potential of the renewable energy resources available on the surface of the globe. This potential has the impact to secure long-term sustainability energy source, diversity in energy resources markets and global atmospheric emissions (Mellit *et al.* 2009). Among the various renewable energy resources, solar energy is ubiquitous and harvested by exploiting the various technologies (Meral and Dinçer 2011). Moreover, this harvested solar energy can be stored and converted to other useable form of energy (thermal or electrical energy).

The harvested solar energy by a collector surface is a complex function of various arguments in different time scales. Some of these influential arguments are local climate, solar radiation intensity, orientation and optical properties of collector surface and radiation reflection properties of ground (Benghanem 2011). The amount of solar energy harvested by collector surface is strongly dependent on collector surface azimuth & inclination angles. The accurate understating and analysis of these influential arguments on the collector surface is of vital importance to harvest the maximum possible energy from the incident radiations (Rustemli *et al.* 2010).

The continued work on solar renewable energy harvesting technologies development and deployment is the need of the hour for developing countries, i.e., Pakistan. Most of the areas in this country exhibit the four-extreme season during the whole year i.e., extreme summer, winter, tropical and autumn. To cope with these harsh environments, reliable and economic solar energy harvesting technologies development is the need of the time. Many researchers have put an effort to study the technical and economic viability for solar collectors and PV panels (Khalid and Junaidi 2013). For the technical side development, factors affecting the insolation harvesting and their proper analysis is a vital task.

In the specialized literature some empirical correlations are proposed to calculate tilt (slope) of collector surface for maximum solar radiation energy. Review of various radiation models and its experimental mapping is reported by (Budiyanto and Lubis 2020) and it

* Corresponding author
Email: nahmad@uet.edu.pk (N. Ahmad)

https://doi.org/10.14710/ijred.2022.38748
ISSN: 2252-4940/© 2022.The Author(s). Published by CBIORE

was concluded that the model proposed by Liu and Jordan shows in a good agreement with the measurement results.

From literature, it is reported that the surfaces oriented towards south with an inclination of 20-30o degrees of angle collects and maximum solar energy (Hussein *et al.* 2004). It is also reported that yearly fixed slope (inclination) of the collector surface should by 5-8o degrees less than the site latitude for enhanced the solar energy (Shariah *et al.* 2002). Duffie *et al*, has proposed the use of (φ ± 15o), plus/minus sign is for the winter and summer season respectively (Duffie and Beckman 2013). Some researchers have suggested a formulation that consists of 12 equations for the calculations of monthly optimal slope angles for latitudes between 60° north and 60° north (Nijegorodov, Devan *et al.* 1994, Gunerhan and Hepbasli 2007).

Kadir et at, has proposed general models for optimum tilt angles of solar panels for Turkey. This optimization of tilt angles was performed using solar radiation measured data for eight big provinces of Turkey (Bakirci 2012). Dike *et al*, had presented the optimal inclination angles (OIA) for PV modules in the absence of a mechanized or automated solar tracking device for optimum yield in solar electricity generation for some selected African cites using photovoltaic geographic information system (PVGES) dataset (Dike *et al.* 2012). Y.P. Chang had exploited the particle swam optimization method in determining the optimal tilt angle of tracking modules in Taiwan. The objective function was to maximize the output energy by using matrix experiments with an orthogonal array with full factorial experiments (Chang 2010).

Single and dual continuous tracking systems are exploited to harvest the maximum possible energy with and without reflectors (Shufat *et al.* 2019). Some researchers have reported the gain of 30-38% and 48% in harvested solar insolation using dual axis solar tracker without mirror reflector and using mirror reflectors respectively (Manosroi *et al.* 2020). To achieve the balance between benefits and short comings of the single axis and double axis tracking system, feasibility study of 1.5 axis tracking is also conducted for energy performance and shading analysis. (Wong *et al.* 2021)

Estimation of received solar radiations for various locations using different tracking surfaces and their validation is reported in many articles. A theory of experimental approach is exploited for the estimation of global solar radiation for the tropical wet climatic region of India and concluded that proposed method exhibits high potential for the monthly average prediction of global solar radiations (Makade *et al.* 2020). Performance modelling of various collector surfaces for radiation harvesting in Monastir city (Tunisia) is reported by (Maatallah *et al.* 2011). For the eastern Mediterranean region of Turkey, estimation of global solar radiation is conducted and its graphical user interface is developed to validate the model data (Yıldırım *et al.* 2018). Global solar radiation modelling for climatic conditions of Mauritius is reported in (Doorga *et al.* 2019) and concluded that daily energy received is about 16MJ/m^2/day.

Above mentioned literature reports the monthly optimal angles, single axis and double axis, selected single option at a time and compared its results with the flat surface and incremental gain in computed. The solar radiation models adopted in this literature for a collector surface use month wise or hourly radiation that is usually used for heating or PV power systems for various specific locations. The objectives of this work are enumerated as follows.

- Development of a comprehensive mathematical model to estimate the instantaneous solar radiation profiles (for any day of the year) incident on horizontal and tracking surface for geographic location of Lahore city, Pakistan.
- Validation of the developed model by comparing the estimated data with the actual data taken from RETScreen (energy management tool) and plot the difference.
- Computation of month wise and yearly insolation received by fixed collector surfaces (horizontal, yearly tilted and monthly tilted) and tracking surfaces (single axis and dual axis) for performance evaluation.

2. Solar Angles and Radiation Modeling

Sun emits total energy of 3.8x10^{20} MW and being the center of our solar system having a diameter of approximately 1.39x10^{9}m. From this huge amount of energy emitted by sun only a tiny amount about 1.7x10^{14} kW is captured by the earth surface that has travelled a mean distance of 1.496x10^{11} m (Kalogirou 2004). The eccentricity of the earth's orbit is such that the distance between the sun and earth varies by 1.7% (Duffie and Beckman 2013). The true anomaly is an angular parameter that defines the position of the earth moving along a Keplerian orbit and is defined as the angle between the direction of the periapsis and the current position of the earth as seen from the sun. The mean anomaly B is parameter relating position and time for the earth moving in a Kepler orbit and it is given by equation (1).

$$B = \frac{360}{365}(n-1) \quad (1)$$

In this equation n is the ordinal date and its value varies from 1 to 365 (according to the day of the year). The measure of angle between solar radiations coming to earth and the plane of earth's equator is called the declination of the sun with respect to earth rotation and is denoted by and is shown in Figure 1. Solar declination can be calculated by equation (2) or (3) (Duffie and Beckman 2013). In these equations, B is mean anomaly of the earth and n is the day of the year.

$$\delta = 0.0069 - 0.3999\cos B + 0.0702\sin B \quad (2)$$

$$\delta = \sin\left(\frac{360}{365}(284+n)\right)23.45^o \quad (3)$$

Figure 1 illustrates the earth-sun angles. The latitude angle is the angle between a line drawn from observer Q on the earth's surface to the center of the earth and the earth's equatorial plane. The hour angle ω is the east or west displacement of sun from local meridian due to rotation of the earth and is taken as per hour. This angle is taken as +ve afternoon and -ve in the dawn and is calculated using equation (4).

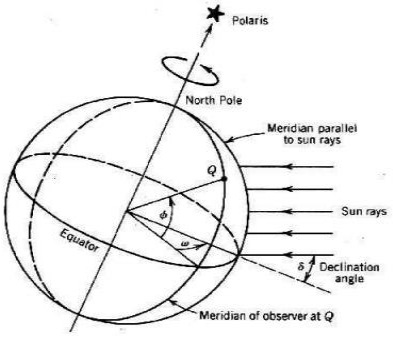

Fig 1. Representation of earth sun angles (Stine and Geyer 2001)

$$\omega = 15(t_s - 12) \tag{4}$$

Solar time t_s is based upon the apparent motion of the sun across the sky. The angles that define the position of the sun in the sky with respect to observer are the zenith angle (θ_z), solar altitude angle (α_s) and solar azimuth angle (γ_s). These angles are shown in Fig 2.

Zenith angle (θ_z) is a function of latitude(φ), hour angle(ω) and solar declination(δ) and is computed using equation (5) (Duffie and Beckman 2013).

$$\theta_z = cos^{-1}(\cos\delta\cos\varphi\cos\omega + \sin\delta\sin\varphi) \tag{5}$$

Fig 2 illustrates the observer sun angles and collector surface angles (surface azimuth angle (γ) and slope (β)). The incident angle (θ) of solar radiations on collector surface is the angle between the beam radiation on a surface and the normal to the surface. This angle is a function of earth sun angles, observer sun angles and collector surface orientation angles and is computed by equation (6) (Duffie and Beckman 2013).

$$\begin{aligned}\cos\theta = {} & \sin\delta\,(\sin\varphi\cos\beta - \cos\varphi\cos\gamma\sin\beta) \\ & + \cos\omega\cos\beta\cos\varphi\cos\delta \\ & + \cos\omega\sin\beta\cos\gamma\sin\varphi\cos\delta \\ & + \sin\omega\cos\delta\sin\beta\sin\gamma\end{aligned} \tag{6}$$

The measure of extra-terrestrial radiation outside the atmosphere is known as the radiation constant. The WRC (world radiation center) has adopted the 1367 W/m^2 value and is widely used for solar energy calculations and is denoted by G_{sc}. The insolation reaching at the top the atmosphere (incident on plane, normal to the radiation) is denoted by G_{on} is computed by (7) (Duffie and Beckman 2013).

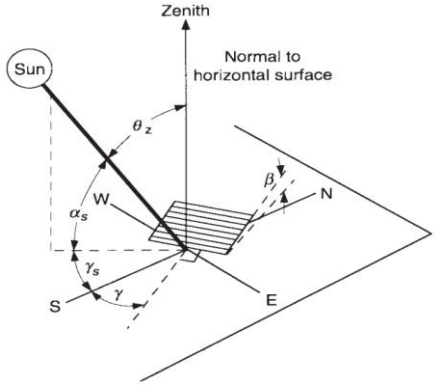

Fig 2. Depiction of solar angles and surface orientation angles (Duffie and Beckman 2013)

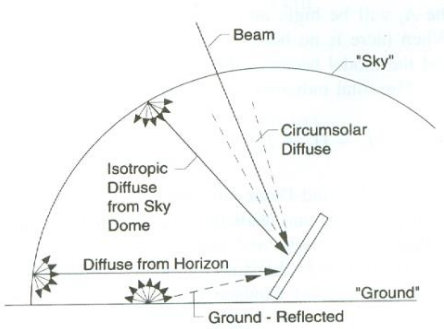

Fig 3. Different components of diffused radiations on inclined surface

$$G_{on} = \begin{Bmatrix} G_{sc}(1.0001 + 0.034221\cos B + 1.0001280\sin B) \\ +0.000719\cos 2B + 0.000077\sin 2B) \end{Bmatrix} \tag{7}$$

G_{oh} is the extra-terrestrial radiation incident upon horizontal surface and it depends on G_{on} and zenith angle (θ_z). It is the amount of solar insolation reaching the surface present just outside the earth's atmosphere and is computed using equation (8).

$$G_{oh} = G_{on}(\cos\theta_z) \tag{8}$$

The radiations incident upon the flat collector surface on earth surface are known as global radiations (denoted by G). These radiations are combined effect of diffused radiations (G_d) and beam radiations (G_b) and described by following expression (9).

$$\overline{G} = \overline{G}_b + \overline{G}_d \tag{9}$$

Hottel *et al,* (Hottel 1976) estimated the beam radiation transmitted through atmosphere without being diffused or scattered by the atmosphere. This model takes zenith angle (θ_z) and altitude (A) into account for all climatic condition i.e., winter, summer, autumn and spring. The (transmittance coefficient) τ_b for beam radiation is computed using expression (10).

$$\tau_b = a_0 + a_1\,exp\left(\frac{-k}{\cos\theta_z}\right) \tag{10}$$

The constants k, a_0 *and* a_1 are computed according to following expression (11). Altitude of the site (A=5km) for Lahore geographic location is considered in this calculation.

$$\begin{aligned} a_0^* &= 0.423 - 0.0082(6 - A)^2 \\ a_1^* &= 0.505 + 0.0059(6.5 - A)^2 \\ k &= 0.271 - 0.0185(2.5 - A)^2 \end{aligned} \tag{11}$$

The diffused radiations G_d is the measure the part of the solar radiations reaching to earth surface after being scattered from the atmosphere by the suspensoid or molecules (Benghanem 2011). The (transmittance coefficient) τ_d for diffused radiation is computed using equation (12) as reported by Liu and Jordan (Duffie and Beckman 2013).

$$\tau_d = 0.270 - 0.295\tau_b = \frac{G_{dh}}{G_{oh}} \tag{12}$$

Mondal et al., estimated the relation between diffused radiation and global radiation by considering the clearness index k (Mondol, Yohanis et al. 2008). This relation is provided in following expression.

$$\frac{G_d}{G} = \begin{cases} 0.98k (k \le 0.2) \\ 0.6109 + 3.625k - 10.171k^2 + 6.389k^3, (0.22 \le k \le 0.8) \\ 0.672 - 0.475k, (k > 0.80) \end{cases} \quad (13)$$

Beam radiations received by the inclined collector is a function of radiations received by horizontal surface and shape factor R_b of collector. Shape factor R_b is computed from the zenith angle (θ_z) and beam ray angle (θ) by using equation (14).

$$R_b = \frac{\cos\theta}{\cos\theta_z} \quad (14)$$

The beam radiations received on tilted collector surface G_{bT} is computed by equation (15).

$$G_{bT} = R_b . G_b = \frac{\cos\theta}{\cos\theta_z} G_b \quad (15)$$

Many authors have computed the diffused component of the solar radiation using three types of the models, these are, isotropic, circumsolar and anisotropic (Li and Lam 2004). Anisotropic model considers the nonuniform distribution of diffused sky radiation in the circumsolar region and uniform distribution from the rest of the sky. The benefit of this model is its adaptability in all climatic condition, that might be cloudy, partly cloudy or clear. HDKR, Hay-Davis-Klucker-Reindell model is exactly based on anisotropic model for solar insolation estimation (Chwieduk 2009). This model incorporates all components of diffused radiations: isotropic, circumsolar and horizontal component. Figure 3 shows these three components of diffused radiations. Using this anisotropic sky model, the diffuse radiations received by tilted collector plate (G_{dT}) is calculated from equation (16).

$$G_{dT} = G_d R_b A_i + G_d \left[1 + f \sin^3\left(\frac{\beta}{2}\right)\right]\left(\frac{1+\cos\beta}{2}\right)(1 - A_i) \quad (16)$$

In this expression, A_i is circumsolar diffused radiation index. This index is function of beam radiation on the ground surface (G_b) to extraterrestrial radiation (G_o) and expressed in equation (17).

$$A_i = \frac{G_b}{G_o} = \frac{G_{bn}}{G_{on}} \quad (17)$$

The f is modulating factor and represents the cloudiness in the atmosphere and given by equation (18)

$$f = \left(\frac{G_b}{G}\right)^{0.5} \quad (18)$$

This radiation model assumes that ground reflected radiations are isotropic, denoted by G_r and is computed by equation (19).

$$G_r = \rho\left(\frac{1-\cos\beta}{2}\right) G \quad (19)$$

In this relation, ρ is surrounding diffused reflectance for total solar radiation.

Total solar radiations received on inclined surface (G_T) is the summation of beam, diffused and reflected radiations and is expressed in the equation (20).

$$G_T = G_{bT} + G_{dT} + G_r \quad (20)$$

Anisotropic sky diffused model used for this case study in its final equation is expressed as (21). (Chwieduk 2009)

$$G_T = R_b(G_b + G_d . A_i) + G_d\left[1 + f\sin^3\left(\frac{\beta}{2}\right)\right]\left(\frac{1+\cos\beta}{2}\right)(1 - A_i) + \rho\left(\frac{1-\cos\beta}{2}\right) G \quad (21)$$

3. Matlab/Simulink Model

The complete radiation model that incorporates, anisotropic sky diffused model, reflected radiations and beam radiations is used for our case study. Its complete simulation model in the MATLAB/Simulink environment is developed. It considers the various input parameters and computes/plots the total radiation received by the tilted surface for a particular day. The arguments for this complete model are the input blocks of solar constant (G_{sc}), Lahore city latitude (φ), year day (n), simulation time (t), surface azimuth (ω_s) and surface slope angle (β). MATLAB function "Declination" accepts the year day (n) and computes the declination of earth (δ) by using equation (1), (2) and (3). The simulation time (t_s) is considered as an argument of function "Hour Angle" and computes the solar azimuth angle (ω) by making use of equation (4). Solar constant (G_{sc}) and year day (n) are processed by function "Normal Extraterrestrial Radiation" and generates the value of (G_{on}).

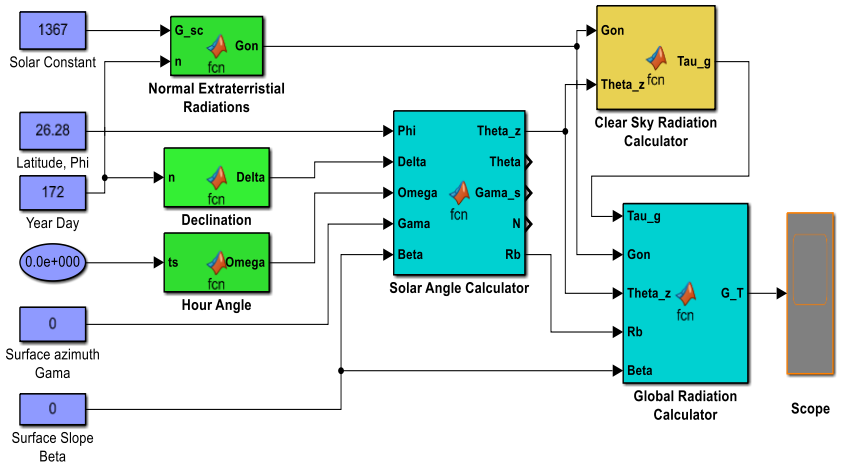

Fig 4. Complete schematic diagram of MATLAB/Simulink model

The function "Solar Angle Calculator" considers the solar angles (declination and hour angle), observer location latitude (φ) and collector surface orientation angles (surface azimuth angle and its slope) as an input parameters and computes the solar zenith angle (θ_z) radiation incidence angle (θ), solar azimuth angle (ω_s), length of day (N) and shape factor (R_b) by implementing the equation (5) and (6). Function block "Clear Sky Radiation Calculator" implements the equation (10), (11) and (12) and computes the transmittance coefficients (τ_b and τ_d). An isotropic model for the global radiation on inclined surface is scripted in block "Global radiation calculator" by using equation (16) to (21). The simulation time for this model is 0-10 seconds and variable type ode45 solver is used. The model is simulated for various days of the year and different combinations of collector surface orientation. For every iteration global radiation data is exported the MATLAB workspace for plotting and performance evaluation purpose. Complete schematic diagram of the developed model is evident in Fig 4.

4. Results and Discussions

The developed model is simulated for Lahore City, situated on eastern region of Islamic republic of Pakistan. The geographical coordinates of Lahore city are 31.5820° N and 74.3293° E with an altitude is 217 meters. Model simulation data in exported to workspace and plotted, solar time is taken as abscissa and global radiation is considered as ordinate in the plots.

4.1. Instantaneous irradiation profiles for various days

Instantaneous solar radiation profiles for various days of the year are generated from the model. Different days of the year, e.g., vernal equinox, summer solstice, autumn equinox and winter solstice (n=80, 172, 266, 356) are considered to analyse the effect of solar insolation received by collector surface. Surface azimuth and slope angle are kept equal to zero for the purpose of simulations. Fig 5 shows the result of radiation profiles for various days of the year.

The sun appearance time in sky is different for winter and summer season. Due to this overall day time fluctuates between 10 hours in winter to about 14 hours in summer solstice day. As each day varies from preceding or succeeding day, the amount of maximum radiation differs. Sun's elevation changes with season and it is maximum in summer season (comprised of May, June, July) and is minimum in winter months (Oct, Nov, Dec and Jan).

4.2. Instantaneous irradiation profiles for different slopes

Solar radiation profile and energy received by solar collector plate is strong function of collector surface slope. The slope of the collector plates is set at 0, 30, 60 and 90 degrees, and solar radiation profiles are generated as shown in Fig 6(a-d). Different extreme days of the year, e.g., autumn equinox, vernal equinox, summer solstice and winter solstice are selected for solar radiation profile generation.

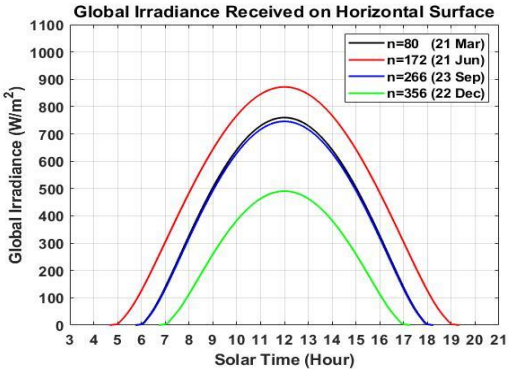

Fig 5. Irradiation profiles for various days

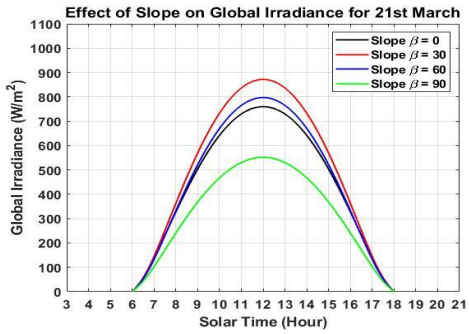

Figure 6a: 21st March, Vernal Equinox Day

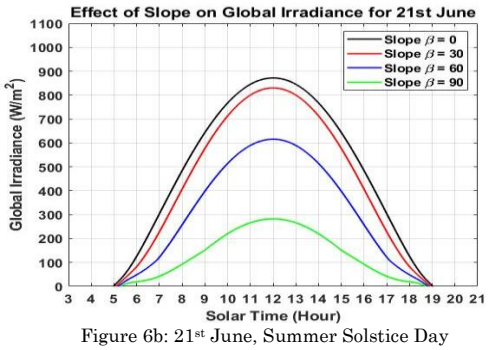

Figure 6b: 21st June, Summer Solstice Day

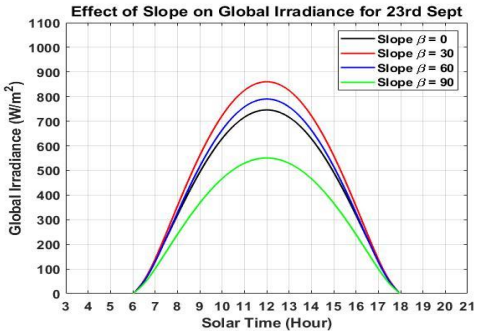

Figure 6c: 23rd Sept, Autumnal Equinox Day

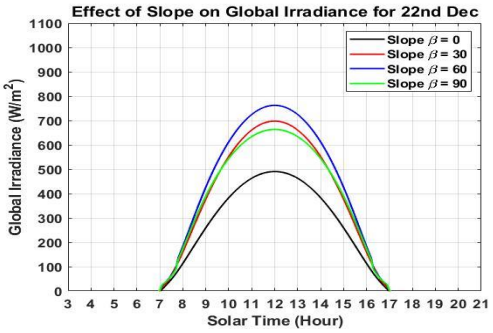

Figure 6d: 22nd Dec, Winter Solstice Day

Fig 6. Instantaneous irradiation with various collector slopes for vernal equinox days(a), summer solstice days(b), autumn equinox day(c) and winter solstice day(d).

On 21st June (summer), day light duration is 14 hours (5.00 to 19.00 solar time) and the peak radiation varies from 290 W/m^2 to 875 W/m^2, when the collector elevation is changed from 0-90 degrees. Obviously, the maximum irradiation is seen when the collector surface elevation is zero, and its reason is that solar zenith angle is almost zero at noon and collector surface harvests the maximum insolation. For slopes of 30, 60 and 90, the maximum irradiation received at noon are 830 W/m^2, 610 W/m^2 and 290 W/m^2 respectively. All these irradiation profiles are evidenced in Fig 6(a-d).

In winter solstice day, the day light duration is 10 hours (7.00 to 17.00 solar time) and the maximum irradiation varies from 500 W/m^2 to 755 W/m^2, when the collector elevation is changed from 0-60 degrees. Obviously, maximum irradiation is seen when the collector surface elevation is 60, and its reason is that solar zenith angle is same as that of collector surface elevation angle (60^o). Further increase in the elevation angle (90^o) curtails the maximum received irradiation and is recorded as 670W/m^2. All the irradiation profiles are evidence in Fig 6(a-d).

In the both equinox days (vernal and autumnal), day light duration is almost 12 hours (6.00 to 18.00 solar time) and the maximum radiation at solar noon is 750 and 740 W/m^2 for horizontal solar collector as shown in Fig 6a,6c. In these days, increase in collector elevation up to 30^o reveals the increase in the insolation and after then it decreases to minimum when the slope of collector is 90.

4.3. Yearly and monthly optimal elevation

The developed model is run for all the days of the year (by keeping the elevation of the solar collector fixed) and cumulative solar insolation is computed. By changing the slope of the surface yearly insolation is recorded in an array and then it is plotted. Yearly received insolation is taken as ordinate and slope of the collector surface is taken as abscissa. Fig 7 reveals yearly insolation as a function of collector slope.

For the horizontal flat surface (when the elevation angle is zero) the received specific insolation is 6900 MJ/m^2 and when the collector inclination is 90^o the insolation decreases to 4600 MJ/m^2. It is evident that the maximum yearly collected insolation is 7600 MJ/m^2, when the collector inclination is 29^o degrees. This observation is according the finding of (Chang 2009). From the results, yearly optimal slope angle is 29 that corresponds to 0.92 times the latitude of the Lahore city (31.5^o).

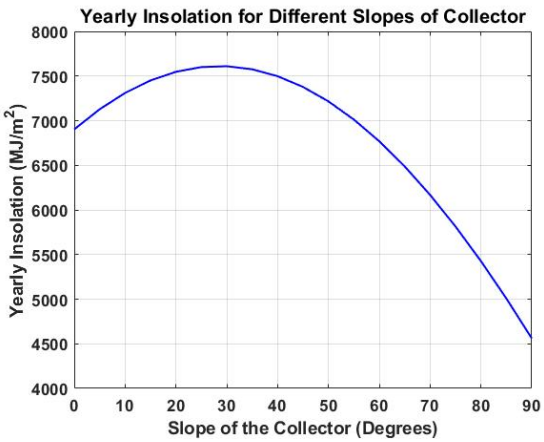

Fig 7. Yearly insolation as a function of collector inclination

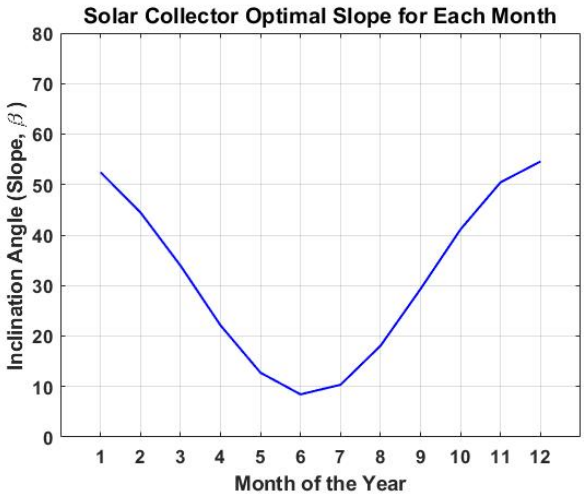

Fig 8. Profile of collector inclination

Due to cost and operational aspects of continuous tracking system, step tracking is proposed by Gunerhann *et al,* (Gunerhan and Hepbasli 2007). The collector surface inclination/slope is adjusted month wise. Monthly adjustment angle is calculated by considering the solar beam radiation angle as zero to the collector surface for the central day of the month. For the Lahore city, optimal tilt angle of the collector surface for each month are computed and it changes form 8.5^o (in June) to 54.6^o (in December). Fig 8 shows the profile of monthly optimal tilt angle for complete year.

4.4. Model validation using RETScreen Data

The developed model in Matlab/Simulink provides the profile of irradiance data v/s solar time, for a particular day in year. The total received energy by collector surface is computed by calculating the area under the profile of the plot. The model is run in iterative method to compute received energy by the solar collector for all days in specific month. Summation of this data provides the monthly received energy. From the Fig 9 it is evident that the minimum specific solar insolation for December is 10.55 MJ/m^2/day and maximum is in June (26.1 MJ/m^2/day).

Another set of monthly insolation for our site is taken from RETScreen program (clean energy management software system). It collects the actual measured data for various locations in the world and is easily accessible through its software. Model data, RETScreen data, their difference and percentage error are shown in Fig 9. The minimum difference between model and actual data is 0.8% in November whereas maximum difference is 21.8% for the month of July. The justification for this difference is the precipitation (rainy over cast season), that hinders the travel of solar radiations to the earth and decreases solar radiation incident on the solar collector. Fig 10 show the profile of %age error and precipitation for Lahore city. It is evident that for the increase in precipitation, insolation is reduced, hence %age error is increased. For the whole year the collected solar insolation is 226.65 MJ/m^2/day and actual is 202.14 MJ/m^2/day having the percentage error of 10.8%.

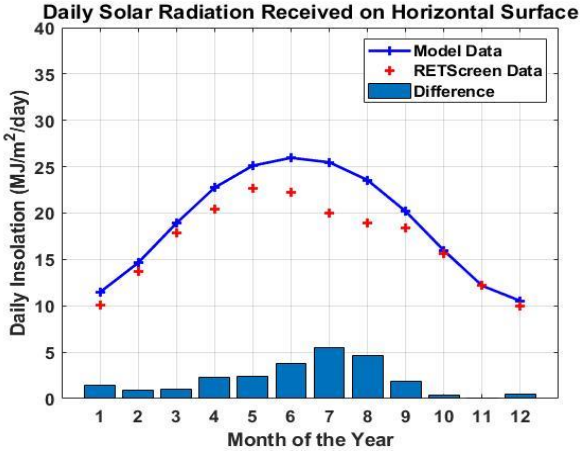

Fig 9. Plot of mean daily solar radiation (Model data, RETScreen data and difference)

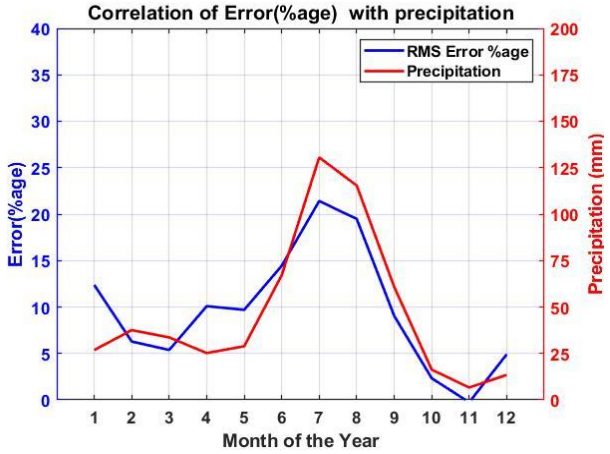

Fig 10. Correlation %age error with precipitation

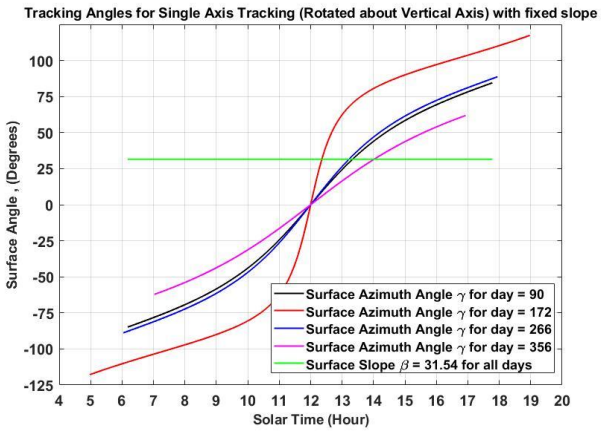

Fig 11. Single axis tracking angles

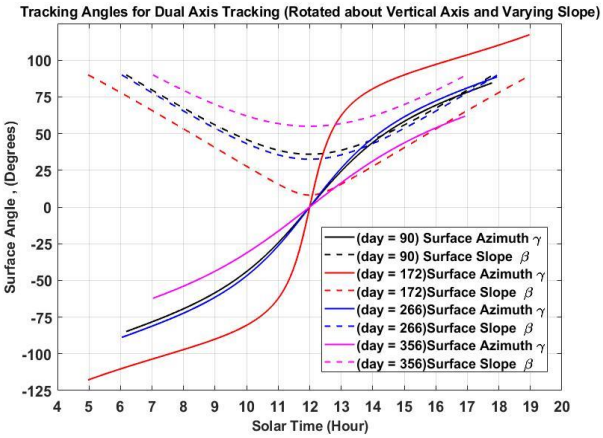

Fig 12. Double axis tracking angles

4.5. Single and dual axis tracking angles

Tracking systems are used for enhanced collection of solar insolation. Each tracker system has a role in the adjustment of the azimuth angle and inclination of the solar collector. The one axe is for the adjustment of elevation or slope of the collector, the other axe is used for vertical rotation to adjust the azimuth angle. For the single axis tracking, inclination of collector surface is kept equal to site latitude (Chang 2009), and the azimuth angle is varied according to the solar azimuth angle.

$\beta = cons\,tan\,t = \varphi$ Collector inclination = Latitude (of Lahore)

$\gamma = \gamma_s$ Collector azimuth angle = Solar azimuth angle

In double axis tracker system both the azimuth angle and the slope of the collector surface are adjusted to keep the beam radiation normal. Four extreme days of the year were selected for the calculation of tracking angles for both, single axis and double axis tracker system. Fig 11 and Fig 12 shows the tracking angles computed for the four extreme days for Lahore city.

4.6. Effect of surface azimuth angle on global irradiance

Surface azimuth angle is an important parameter that effects the instantaneous irradiation reaching the collector. To analyse the effect of surface azimuth angle (elevation angle of collector surface is kept equal to 31.5°) on the instantaneous irradiation, three values of collector azimuth angle -60, zero and 60 are considered in all simulation cases. Fig 13(a-d) shows the instantaneous irradiation reaching the collector surfaces for four days of the year for various azimuth angles.

In summer solstice day (22nd June), the day light duration is 14 hours (5.00 to 19.00 solar time) and the maximum irradiation 810W/m² is received at solar noon, when the collector azimuth angle is kept at 0° in simulation. When the solar azimuth angle is set at -60° (oriented towards east), solar radiation profiles is shifted towards left of the solar noon in the plot and maximum received irradiation is 855W/m² at 10.30 solar time. In the simulation, for the solar azimuth angle of +60° (oriented towards west), solar radiation profile is shifted towards right of the solar noon in the plot and maximum received irradiation is 855W/m² at 13.30 solar time. This shift in the irradiation profile and increase in its maximum value is attributed to the timing of the sun in the horizon, when the solar radiations are normal to the collector surface. All these irradiation profiles are evidenced in Fig 13(a-d).

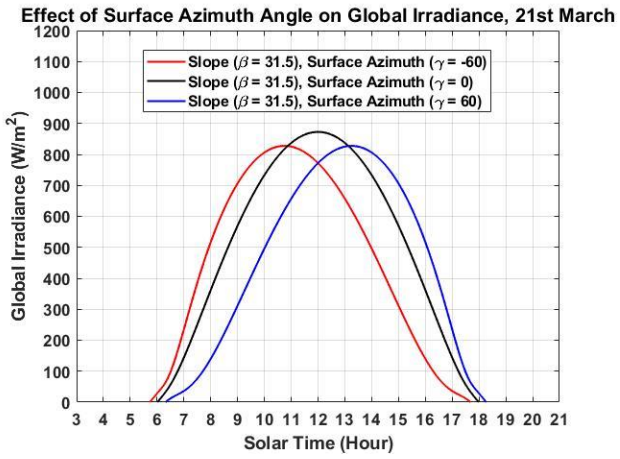

Figure 13a: 21st March, Vernal Equinox Day

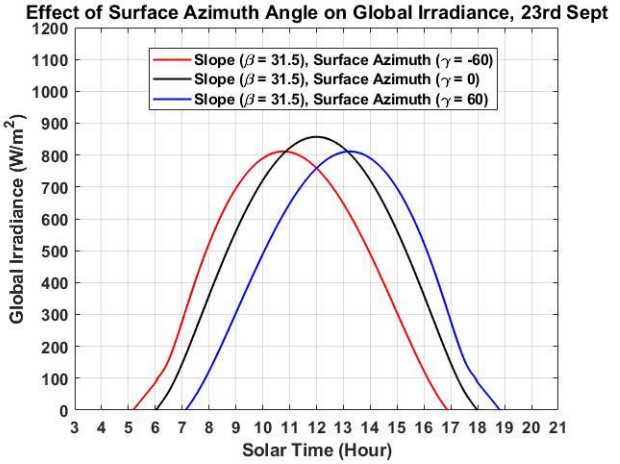

Figure 13c: 23rd Sept, Autumnal Equinox Day

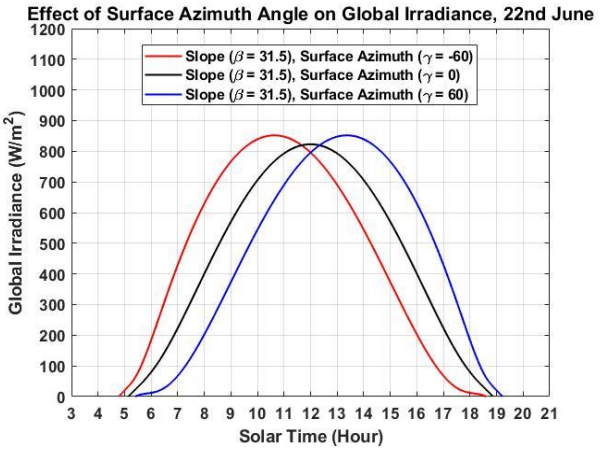

Figure 13b: 22nd June, Summer Solstice Day

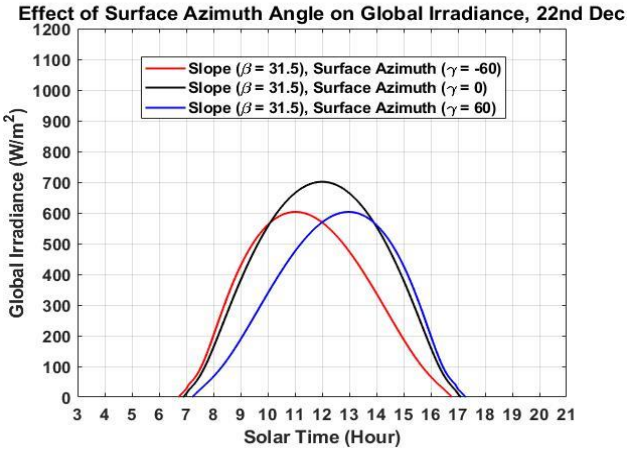

Figure 13d: 22nd Dec, Winter Solstice Day

Fig 13. Instaneneous irradiation with differnet collector azimuth angles during vernal equinix days(a), summer solstise days(b), autumn equinox day(c), and winter solstice day(d).

In winter solstice day (22nd Dec), the day light duration is almost 10 hours (7.00 to 17.00 solar time), for the collector azimuth angle as 0° degrees, the maximum irradiation of 700W/m² is received at solar noon. When the solar azimuth angle of -60° and +60° is set, solar radiation profile is shifted towards left and right of the solar noon respectively and the maximum received irradiation is 600W/m² in both cases. This decrease in maximum solar irradiation is attributed to increase in solar radiation incidence angle and it is due to high solar zenith angle and low inclination angle of the collector plate. All these solar profiles plots are shown in Fig 13(a-d).

In the both equinox days (21st Mar and 23rd Sept), the day light duration is almost 10 hours (7.00 to 17.00 solar time), for the collector azimuth angle as 0° degrees, the maximum irradiation of 870W/m² is received at solar noon. For the solar azimuth angle of -60° and +60°, solar radiation profile is shifted towards left and right of the solar noon respectively and the maximum received irradiation is 810W/m² in both cases. This decrease in peak solar irradiation is attributed to increase in solar radiation incidence angle at that time. All solar irradiation profiles for both equinox days are evidences in Fig 13a and Fig 13d.

4.7. Analysis of received insolation for fixed and tracking collector surfaces

So far as we have developed comprehensive model and simulated it for various fixed and tracking options. In fixed options we have flat plat, yearly optimal tilt and monthly optimally tilt options. Where as in continuously tracking options, single axis and double axis considerations are simulated. A comprehensive model is developed that encompasses all operational modes (fixed and tracking) of collector and provides received insolation profiles in single plot for evaluation and comparison purpose. Fig 14 shows the received insolation for various configurations of collector for four extreme days of the year for Lahore city. Single run of the model provides the insolation profile for one day only. The received insolation by collector surface is computed by calculating the area under the radiation profile curve. To compute the yearly received insolation for all configurations of the collector, the model was run in 365 iterations and the data was stored in an array having order of 365 x 5. Each row corresponds to the day of the year and each column represent the collector configurations (flat, yearly tilt, monthly tilt, single axis and dual axis). Monthly received insolation is computed by taking the sum of the selected elements of the array for all configurations. Table 1 summarizes the collected solar radiation energy for

different fixed and tracked collector surfaces and percentage gains for each month and for whole year. For the single and dual axis tracking surfaces, yearly harvested energy is 8843MJ/m^2 and 9374MJ/m^2 respectively and this figure is 30% and 37% more as compared to the horizontal surface. If the insolation received by yearly optimal tilt is considered as reference value, then energy gain for monthly optimal tilt, single axis and double axis is recorded as 5%, 19% and 27% respectively.

5. Conclusion

In this work site specific detailed modeling of solar radiation for Lahore city, Pakistan is conducted. The developed model is programmed in Simulink/Matlab environment for its simulation and solar radiation profile generation. This model accepts the solar constant, site latitude & longitude, year day, collector plate azimuth & slope angles as arguments and computes the solar radiation energy profiles. The model is simulated for various extreme days of the year and attained the solar radiation profile. The model is also set to run for 365 days (for the whole year) and month wise harvested energy is calculated. These results are then compared with real data of the Lahore city site (attained from the RETScreen) for the validation of developed model. This validated model is then used for the performance analysis of various fixed and tracked surfaces for this city. Some remarks are listed below.

- The developed model is simulated and validated with the experimental data based upon the monthly received insolation for flat plat collector. The minimum difference between model and actual data is 0.8% in November whereas maximum difference is 21.8% for the month of July. This increased error in July is due to the high precipitation (rainy over cast season), that hinders the travel of solar radiations to the earth and decreases solar radiation incident on the solar collector plats. For the whole year the collected solar insolation is 226.65MJ/m2/day and actual is 202.14MJ/m2/day and the percentage error is 10.8%.
- The yearly optimal tilt angle of collector surface for Lahore city is 29.1o faced due south and it is 0.92 times the latitude of the site (31.5 o). For the yearly tilted surface, as compared to with the flat surface, the maximum and minimum gain in the insolation is for the month of December and June and is 42% and -11% respectively. Yearly insolation gain made by collector surface having the yearly optimal tilt panels is 8% higher than the flat collector for Lahore city.

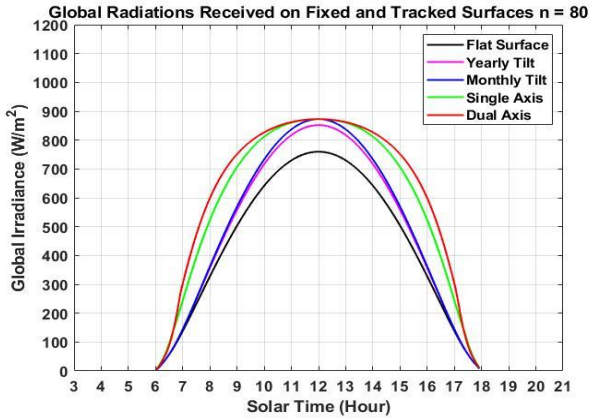

Figure 14a: 21st March, Vernal Equinox day

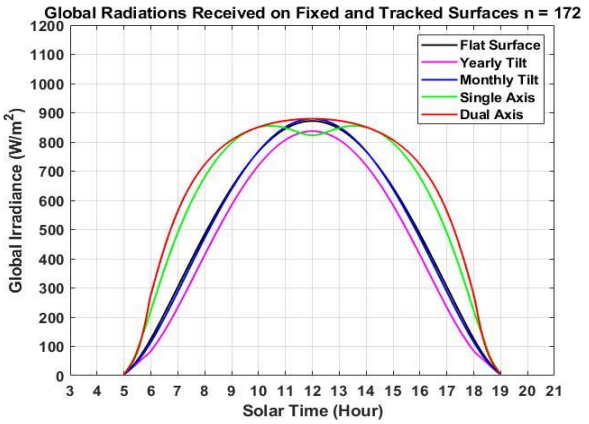

Figure 14b: 21st June, Summer Solstice day

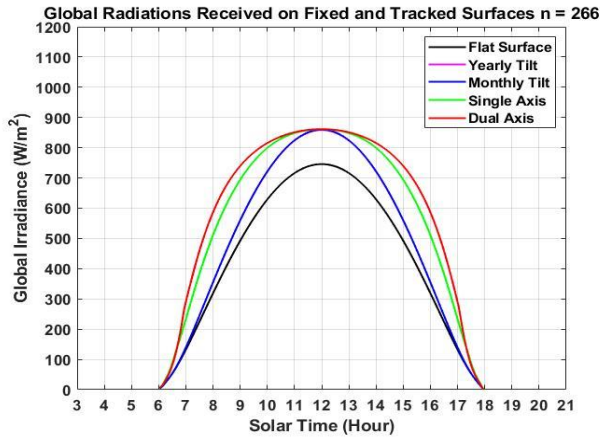

Figure 14c: 23rd Sept, Autumnal Equinox day

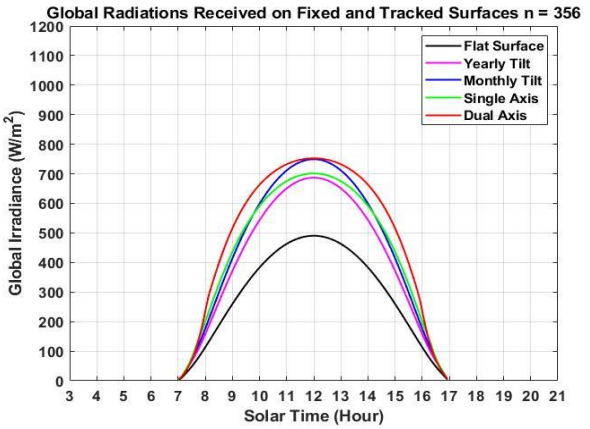

Figure 14d: 22nd Dec, Winter Solstice day

Fig 14. Instantaneous irradiation profiles with various fixed and tracking collector surfaces for vernal equinox days(a), summer solstice days(b), autumn equinox day(c), and winter solstice day(d).

Table 1
Monthly and yearly received insolation by fixed and tracked surfaces

Month	Horizontal Collector (MJ/m²)	Yearly Tilt (MJ/m²)	%age (Ref FlatPlate)	Monthly Tilt (MJ/m²)	%age (Ref FlatPlate)	Single Axis (MJ/m²)	%age (Ref FlatPlate)	Dual Axis (MJ/m²)	%age (Ref FlatPlate)
January	355	492	38%	524	47%	528	49%	581	64%
February	405	518	28%	532	32%	570	41%	612	51%
March	572	656	15%	657	15%	754	32%	792	38%
April	666	678	2%	690	4%	826	24%	861	29%
May	765	711	-7%	763	0%	920	20%	962	26%
June	767	682	-11%	760	-1%	912	19%	957	25%
July	778	706	-9%	773	-1%	929	19%	974	25%
August	729	716	-2%	742	2%	897	23%	937	29%
September	606	668	10%	669	10%	787	30%	825	36%
October	495	617	25%	627	27%	690	39%	737	49%
November	365	497	36%	525	44%	537	47%	588	61%
December	326	463	42%	499	53%	493	51%	547	68%
Yearly Comp (based on Flat Plate)	6828	7405	8%	7761	14%	8843	30%	9374	37%
Yearly Comp (Based on Yearly Optimal Tilt)	--	7405	0%	7761	5%	8843	19%	9374	27%

ISSN: 2252-4940/© 2022. The Author(s). Published by CBIORE

- Optimal inclination/slope for each month for solar collector installed at Lahore city, are also computed. The maximum tilt is 54.6o for December and it decreases gradually for each month and approaches the minimum value of 8.4o for the month of June. For a monthly, insolation received by tilted surface, as compared to with the flat surface, the maximum and minimum gain in the insolation is for the month of December and July and is 53% and -1% respectively. Yearly insolation gain by collector surface having the monthly optimal tilt surface is 14% higher than the conventional flat plate collector for Lahore city.
- Single axis (azimuth type, fixed inclination) is investigated by plotting its tracking angle for whole day, by taking slope angle of the collector surface same as latitude of the selected site. For a single axis tracker surface, received insolation as compared to flat surface, the maximum and minimum gain in the insolation is observed for winter and summer season and is 51% and 19% respectively. Yearly insolation gain for this tracker is estimated as 30% (with flat surface value as reference).
- The insolation gain made by double axis tracker relative to flat surface collector is 25 % and 68 % in the summer and winter solstice days respectively. Moreover, yearly insolation gain by this type of tracking surface is estimated to be 37 % relative to flat plate configuration.
- Cost involved in the installation of autonomous solar radiation collection system are the key factor that are crucial to calculate before its installation so that the Life Cycle Costing (LCC) can be estimated for both options i.e., with or without tracker system facility. This study, based on modelling and simulation provides the information about Lahore locality to adopt the yearly and monthly optimal tilt as well as single/double axis continuous tracking for heat collection system. Based on study and results it is now clear that tracker system has enormous efficiency improvement for heat collection throughout the year for Lahore. Again, the actual decision is based on LCC and overall cost involved in developing and deploying this system.
- This work provides the comprehensive guide line for the researchers, photovoltaic system designers for solar system applications. Such a detailed model, its simulation, insolation data profile generation and performance analysis are not conducted yet for this region especially Lahore. During the discussion with various stake holders from industry and governmental agencies various questions about the performance of fixed and tracked surfaces were raised. In pursuance of these answers this study is conducted and it will provide the guide line for solar system designers. This research will be further expanded with the integration of PV models, grid interactive inverters for smart grid interfacing and electrical power sharing.

Nomenclature

B	Mean anomaly of the earth
G_{sc}	Solar constant, energy from the sun per unit time received on a unit area of surface perpendicular of the radiation outside the atmosphere.
G_{on}	Extraterrestrial radiation incident on the plane normal to the radiation (outside the atmosphere)
G_{oh}	Horizontal extraterrestrial radiation, amount of radiation received on the horizontal surface on the tip of the atmosphere.
G_{dh}	Diffused radiation received on horizontal collector at earth surface
G_{oh}	Radiation received on horizontal collector at outside earth's atmosphere
G_{bT}	Beam radiations received on tilted collector plate
G_{dT}	Diffused radiations received on tilted collector plate
G_{bn}	Beam radiations incident upon surface normal to radiations
G_b	Beam radiations incident upon horizontal flat collector surface
G_d	Diffused radiations incident upon horizontal flat collector surface
G_o	Extraterrestrial radiation incident upon horizontal surface
G	Global radiations incident upon horizontal flat collector surface
G_r	Ground reflected radiations
G_T	Total radiations received on inclined surface
R_b	Shape factor of collector plate
n	Day of the year
t_s	Solar time, it is based on the apparent angular motion of the sum across the sky with solar noon the time the sun crosses the meridian of the observer.
k	clearness index
A_i	Circumsolar diffused radiation index
f	Modulating factor used to represent the cloudiness in the atmosphere
A	Altitude of the site (A=5km) for Lahore geographic location.

Greek Symbol

δ	Declination, angular position of the sun at solar noon w.r.t the plane of the equator
ω	Hour angle, angular displacement of the sun east or west of the local meridian
θ_z	Zenith angle, the angle between vertical and the line to the sun.
α_s	Solar altitude angle, the angle between the horizontal and the line to the sun.
γ_s	Solar azimuth angle, the angular displacement from south of the projection of beam radiation on the horizontal plane.
θ	Angle of incidence, the angle between the beam radiation on a surface and the normal to the surface
φ	Latitude angle, used to describe the location of the observer at earth surface
γ	Collector surface azimuth angle,
β	Slope of collector surface, the angle between the plane of the surface in question and the horizontal.
τ_b	Transmittance coefficient for beam radiations.
τ_d	Transmittance coefficient for diffused radiations.
ρ	Surrounding diffused reflectance for total solar radiations

Subscripts

o	refers to radiation above the earth's atmosphere, extraterrestrial radiation.
b	beam radiation
d	diffused radiation
T	radiation on tilted plane
n	radiation on a plane normal to the direction of propagation

Acknowledgments

The author would like to acknowledge the support of University of Engineering and Technology through mechanical engineering dept by providing computational facility for simulation of the model.

References

Bakirci, K. (2012). General models for optimum tilt angles of solar panels: Turkey case study. *Renewable and Sustainable Energy Reviews* **16**(8), 6149-6159, DOI: https://doi.org/10.1016/j.rser.2012.07.009.

Benghanem, M. (2011). Optimization of tilt angle for solar panel: Case study for Madinah, Saudi Arabia. *Applied Energy* **88**(4), 1427-1433, DOI: https://doi.org/10.1016/j.apenergy.2010.10.001.

Budiyanto, M. A. and Lubis, M. H. (2020). Physical reviews of solar radiation models for estimating global solar radiation in Indonesia. *Energy Reports* **6**, 1206-1211, DOI: https://doi.org/10.1016/j.egyr.2020.11.053.

Chang, T. P. (2009). Output energy of a photovoltaic module mounted on a single-axis tracking system. *Applied Energy* **86**(10), 2071-2078, DOI: https://doi.org/10.1016/j.apenergy.2009.02.006.

Chang, Y.-P. (2010). Optimal the tilt angles for photovoltaic modules in Taiwan. *International Journal of Electrical Power & Energy Systems* **32**(9), 956-964, DOI: https://doi.org/10.1016/j.ijepes.2010.02.010.

Chwieduk, D. A. (2009). Recommendation on modelling of solar energy incident on a building envelope. *Renewable Energy* **34**(3), 736-741, DOI: https://doi.org/10.1016/j.renene.2008.04.005.

Dike, V. N., Chineke, T. C., Nwofor, O. K., and Okoro, U. K. (2012). Optimal angles for harvesting solar electricity in some African cities. *Renewable Energy* **39**(1), 433-439, DOI: https://doi.org/10.1016/j.renene.2011.08.001.

Doorga, J. R. S., Rughooputh, S. D. D. V. and Boojhawon, R. (2019). Modelling the global solar radiation climate of Mauritius using regression techniques. *Renewable Energy* **131**, 861-878, DOI: https://doi.org/10.1016/j.renene.2018.07.107.

Duffie, J. A. and W. A. Beckman (2013). Solar engineering of thermal processes, John Wiley & Sons.

Gunerhan, H. and Hepbasli, A. (2007). Determination of the optimum tilt angle of solar collectors for building applications. *Building and Environment* **42**(2), 779-783, DOI: https://doi.org/10.1016/j.buildenv.2005.09.012.

Hottel, H. C. (1976). A simple model for estimating the transmittance of direct solar radiation through clear atmospheres. *Solar Energy* **18**(2), 129-134, DOI: https://doi.org/10.1016/0038-092X(76)90045-1.

Hussein, H. M. S., Ahmad, G.E. and El-Ghetany, H.H. (2004). Performance evaluation of photovoltaic modules at different tilt angles and orientations. *Energy Conversion and Management* **45**(15), 2441-2452, DOI: https://doi.org/10.1016/j.enconman.2003.11.013.

Kalogirou, S. A. (2004). Solar thermal collectors and applications. *Progress in Energy and Combustion Science* **30**(3), 231-295, DOI: https://doi.org/10.1016/j.pecs.2004.02.001.

Khalid, A. and Junaidi, H. (2013). Study of economic viability of photovoltaic electric power for Quetta – Pakistan." *Renewable Energy* **50**: 253-258, DOI: https://doi.org/10.1016/j.renene.2012.06.040.

Li, D. H. W. and Lam, J.C. (2004). Predicting solar irradiance on inclined surfaces using sky radiance data. *Energy Conversion and Management* **45**(11), 1771-1783, DOI: https://doi.org/10.1016/j.enconman.2003.09.020.

Maatallah, T., El Alimi, S., and Nassrallah, S.B. (2011). Performance modeling and investigation of fixed, single and dual-axis tracking photovoltaic panel in Monastir city, Tunisia. *Renewable and Sustainable Energy Reviews* **15**(8): 4053-4066, DOI: https://doi.org/10.1016/j.rser.2011.07.037.

Makade, R. G., Chakrabarti, S., Jamil, B. and Sakhale, C. N. (2020). Estimation of global solar radiation for the tropical wet climatic region of India: A theory of experimentation approach. *Renewable Energy* **146**, 2044-2059, DOI: https://doi.org/10.1016/j.renene.2019.08.054.

Manosroi, W., Prompattra, P., and Kerngburee, P. (2020). Performance improvement of two-axis solar tracking system by using flat-mirror reflectors. *Energy Reports* **6**, 9-14, DOI: https://doi.org/10.1016/j.egyr.2020.10.029.

Mellit, A., Kalogirou, S.A., Hontoria, L. and Shaari, S. (2009). Artificial intelligence techniques for sizing photovoltaic systems: A review. *Renewable and Sustainable Energy Reviews* **13**(2), 406-419, DOI: https://doi.org/10.1016/j.rser.2008.01.006.

Meral, M. E. and Dinçer, F. (2011). A review of the factors affecting operation and efficiency of photovoltaic based electricity generation systems. *Renewable and Sustainable Energy Reviews* **15**(5), 2176-2184, DOI: https://doi.org/10.1016/j.rser.2011.01.010.

Mondol, J. D., Yohanis, Y. G. and Norton, B. (2008). Solar radiation modelling for the simulation of photovoltaic systems. *Renewable Energy* **33**(5), 1109-1120, DOI: https://doi.org/10.1016/j.renene.2007.06.005.

Nijegorodov, N.,. Devan, K. R. S., Jain, P. K. and Carlsson, S. (1994). Atmospheric transmittance models and an analytical method to predict the optimum slope of an absorber plate, variously oriented at any latitude. *Renewable Energy* **4**(5), 529-543, DOI: https://doi.org/10.1016/0960-1481(94)90215-1.

Rustemli, S., Dincadam, F. and Demirtas, M. (2010). Performance comparison of the sun tracking system and fixed system in the application of heating and lighting. *Arabian Journal for Science & Engineering (Springer Science & Business Media BV)* **35**.

Shariah, A., Al-Akhras, M. A. and Al-Omari, I. A. (2002). Optimizing the tilt angle of solar collectors.*Renewable Energy* **26**(4), 587-598, DOI: https://doi.org/10.1016/S0960-1481(01)00106-9.

Shufat, S. A. A., E. Kurt and A. Hancerlioğulları (2019). Modeling and Design of Azimuth-Altitude Dual Axis Solar Tracker for Maximum Solar Energy Generation. *International Journal of Renewable Energy Development*, **8**(1) 7-13, DOI: 10.14710/ijred.8.1.7-13.

Stine, W. and M. Geyer (2001). Power From The Sun. http://www.powerfromthesun.net/index.html

Wong, J., Bai, F., Saha, T. K. and Tan, R. H. G. (2021). A feasibility study of the 1.5-axis tracking model in utility-scale solar PV plants. *Solar Energy* **216**, 171-179, DOI: https://doi.org/10.1016/j.solener.2020.12.035.

Yıldırım, H. B., Çelik, Ö., Teke, A. and Barutçu, B. (2018). Estimating daily Global solar radiation with graphical user interface in Eastern Mediterranean region of Turkey. *Renewable and Sustainable Energy Reviews* **82**, 1528-1537, DOI: https://doi.org/10.1016/j.rser.2017.06.030.